Full Rescue of F508del-CFTR Processing and Function by CFTR Modulators can be Achieved by Removal of Two Unique Regulatory Regions.

Inna Uliyakina[1], Ana C Da Paula[1], Sara Afonso[1], Miguel J Lobo[1], Verónica Felício, Hugo M Botelho, Carlos M Farinha, Margarida D Amaral*

University of Lisboa, Faculty of Sciences, BioISI – Biosystems & Integrative Sciences Institute, Lisboa, Portugal.

Short title: Role of regulatory extension on CFTR stability.

[1]Current addresses: Department of Physiology, Anatomy and Genetics, University of Oxford, UK (IU and MJL); Novartis Pharmaceuticals, Montreal, Quebec, Canada (ACDP); Department of Physiology, University of Regensburg, Germany (SA).

*Correspondence to:

Prof. Margarida D Amaral

University of Lisboa, Faculty of Sciences, BioISI – Biosystems & Integrative Sciences Institute

Campo Grande, 1749-016 Lisboa, Portugal

Tel: +351-21-750 08 61; Fax: +351-21-750 00 88; Email: mdamaral@fc.ul.pt

Keywords: ABC transporters; cystic fibrosis transmembrane conductance regulator (CFTR); drug action; regulatory extension; regulatory insertion

Supporting Information: Additional figures with supplementary data

#

Abstract

Background and Purpose: Cystic Fibrosis (CF) is caused by mutations in the CF Transmembrane conductance Regulator (CFTR), the only ABC transporter functioning as a channel. Unique to CFTR are two highly conformationally dynamic regions: the regulatory extension (RE) and regulatory insertion (RI). Removal of the latter rescues the trafficking defect of CFTR with F508del, the most common CF-causing mutation.

We aimed here to assess the impact of RE removal (alone or with RI or genetic revertants) on F508del-CFTR traffic and how CFTR modulator drugs corrector VX-809/lumacaftor and potentiator VX-770/ivacaftor rescue these combined variants so as to gain insight into the mechanism of action (MoA) of these drugs.

Experimental Approach. We generated ΔRE and ΔRI CFTR variants (with and without genetic revertants) by site-directed mutagenesis and used them to stably transfect BHK cell lines. We studied CFTR expression and stability by Western blotting and pulse-chase respectively, plasma membrane levels by cell surface biotinylation and channel activity by the iodide efflux technique.

Key Results. Our data demonstrate that ΔRI significantly enhanced rescue of F508del-CFTR by VX-809. Thus, while the presence of the regulatory insertion seems to be precluding full rescue of F508del-CFTR processing by VX-809, this region appears essential to rescue its function by VX-770, thus suggesting some contradictory role in rescue of F508del-CFTR by these two modulators. Nevertheless, this negative impact of RI removal on VX-770-stimulated currents on F508del-CFTR can be compensated by deletion of the regulatory extension which also leads to the stabilization of this mutant. We thus propose that, despite both these regions being conformationally active, RI precludes F508del-CFTR processing while RE affects mostly its stability and channel opening.

Introduction

Cystic Fibrosis (CF), a life-threatening recessive disorder affecting ~80,000 individuals worldwide, is caused by mutations in the gene encoding the CF transmembrane conductance regulator (CFTR) protein present at the apical membrane of epithelial cells. This is the only member of the ATP-binding cassette (ABC) transporter family, functioning as a channel, actually a cAMP-dependent chloride (Cl^-)/ bicarbonate (HCO_3^-) channel. It consists of two membrane-spanning domains (MSD1/2), two nucleotide binding domains (NBD1/2) and a cytoplasmic regulatory domain (RD), which is unique to CFTR[1]. The MSDs are linked via intra- and extra-cellular loops (ICLs, ECLs, respectively). ATP binding promoting NBD1:NBD2 dimerization and subsequent phosphorylation of RD at multiple sites lead to channel gating[2]. The NBD1:NBD2 and ICL4:NBD1 interfaces were shown to represent critical folding conformational sites [3–5] important for the gating and maturation of the CFTR protein [5,6].

Although >2,000 CFTR gene mutations were reported (http://www.genet.sickkids.on.ca/cftr/app), one mutation F508del occurs in 85% of CF patients. This NBD1 mutant fails to traffic to the plasma membrane (PM) due to protein misfolding and retention by the endoplasmic reticulum quality control (ERQC) that targets it to premature proteasomal degradation. F508del-CFTR folding is a complex and inefficient process but it can be rescued, at least partially, by several treatments. These include low temperature incubation[7], genetic revertants[4,5,8–13] or pharmacological agents, like "corrector" VX-809 (lumacaftor)[14], one of the first CFTR modulator drugs to receive FDA-approved in combination with potentiator VX-770/ivacaftor[1]. Determining the additive/ synergistic rescue of F508del-CFTR by small molecules correctors together with other rescuing agents/revertants is very valuable to determine the mechanism of action (MoA) of these CFTR modulators[5].

Comparative studies of CFTR with other ABC transporters are very powerful to understand the uniqueness of some of its regions, their influence on CFTR maturation and function as well as how they affect distinctive binding of CFTR to modulator drugs. Two such unique regions are present in NBD1 of CFTR, which are absent in NBDs of other ABC transporters (Fig.S1) - the regulatory extension (RE) and regulatory insertion (RI). Both regions were described as highly conformationally dynamic[3,16] following PKA phosphorylation at certain (^{660}Ser, ^{670}Ser; ^{422}Ser)[18,19]. Importantly, removal the 32-amino acid RI (ΔRI) was reported to rescue traffic of F508del-CFTR[13].

Our first goal here was to assess the impact of removing the 30-amino acid RE (ΔRE) alone or jointly with ΔRI on the traffic of F508del-CFTR. Secondly, we aimed to evaluate how RE and or RI removal from F508del-CFTR influences the rescue of this mutant by genetic revertants. Our third and final

[1] www.fda.gov/NewsEvents/Newsroom/PressAnnouncements/ucm453565.htm

#

goal was to determine how the traffic and function of these combined variants of F508del-CFTR (ΔRE, ΔRI plus genetic revertants) are rescued by CFTR modulator drugs VX-809 (corrector) and VX-770 (potentiator) to gain further insight into their MoA.

Our data show that although F508del-CFTR without RE did not traffic to the PM, it showed a dramatic stabilization of its immature form (evidencing a turnover rate ~3 x lower than that of wt-CFTR, being the turnover of F508del-CFTR itself is 2x faster vs. wt-CFTR). Results also show that, while ΔRI further increased processing of F508del-CFTR with revertants to almost wt-CFTR levels, RE removal completely abolished their processing, thus highlighting the different impact of the two dynamic regions on revertant-rescued F508del-CFTR. Most strikingly, although VX-809 rescued ΔRI-F508del-CFTR and ΔRE-ΔRI-F508del-CFTR processing to wt-CFTR levels, nevertheless to achieve maximal function of F508del-CFTR, removal of just RI was insufficient, as both RI and RE had to be absent from F508del-CFTR. These data indicate that removal of these two regions has a positive effect on the rescuing efficacy of F508del-CFTR by CFTR modulators.

#

Methods

CFTR variants, cells and culture conditions

Several CFTR deletion variants were produced by site-directed mutagenesis corresponding to the removal of residues: ΔRI_L – ^{404}Gly-Leu^{435}; ΔRI_S –^{412}Ala-Leu^{428}; ΔRE_L –^{647}Cys-Ser^{678}; ΔRE_S –^{654}Ser-Gly^{673}; ΔH9 –^{637}Gln-Gly^{646}; ΔRE_L-ΔH9 –^{637}Gln-Ser^{67}8; ΔRI_S-ΔRE_S –both ^{412}Ala-Leu^{428} and ^{654}Ser-Gly^{673}; and ΔRI_L-ΔRE_S – ^{405}Gly-Leu^{435} and ^{654}Ser-Gly^{673}. All the constructs were produced using full length wt-CFTR and F508del-CFTR.

BHK cells lines expressing ΔRI_L-, ΔRI_L-F508del-, ΔRI_L-G550E-, ΔRI_L-G550E-F508del, ΔRI_L-R1070W-, ΔRI_L-R1070W-F508del, ΔRI_S-, ΔRI_S-F508del, ΔRI_S -G550E-, ΔRI_S-G550E-F508del, ΔRI_S-R1070W-, ΔRI_S-R1070W-F508del, ΔRE_S-, ΔRE_S-F508del, ΔRE_S-G550E, ΔRE_S-G550E-F508del, ΔRE_S-R1070W-, ΔRE_S-R1070W-F508del, ΔRE_L-, ΔRE_L-F508del, ΔRI_S-ΔRE-, ΔRI_S-ΔRE_S-F508del, ΔRI_L-ΔRE-, ΔRI_L-ΔRE_S-F508del, ΔH9-, ΔH9-F508del, ΔRE_L-ΔH9-, ΔRE_L-ΔH9-F508del-CFTR were produced and cultured as previously described [11]. Cells were cultured in DMEM/F-12 medium containing 5% (v/v) FBS and 500μM of methotrexate. For some experiments, cells were incubated with 3μM VX-809 or with the equivalent concentration of DMSO (Control) for 48h at 37ºC.

Western blot

To study the effect of removal of regulatory extension (RE) and or regulatory insertion (RI) in combination with genetic revertants and VX-809, cells were incubated for 48h at 37ºC with 3μM VX-809. After incubation, cells were lysed and extracts analysed by Western blot (WB) using the anti-CFTR antibody (Ab) 596 or anti-calnexin Ab as a loading control. Score corresponds to the percentage of band C to total CFTR (bands B+C) as normalized to the same ratio in samples from wt-CFTR expressing cells. Blot images were acquired using BioRad ChemiDoc XRC+ imaging system and band intensities were measured using Image Lab analysis software.

Pulse-chase and immunoprecipitation

BHK cells lines stably expressing CFTR variants were starved for 30 min in methionine-free α-modified Eagle's medium or minimal essential medium and then pulsed for 30min in the same medium supplemented with 100μCi/ml [^{35}S]methionine. After chasing for 0, 0.5, 1, 1.5, 2 and 3h in a-modified Eagle's medium with 8% (v/v) fetal bovine serum and 1mM non-radioactive methionine, cells were lysed in 1ml of RIPA buffer [1% (w/v) deoxycholic acid, 1% (v/v) Triton X-100, 0.1% (w/v) SDS, 50mM Tris, pH7.4, and 150mM NaCl]. The immunoprecipitation (IP) was carried out using the

#

anti-CFTR antibody in independent experiments and Protein G–agarose or Protein A–Sepharose beads. Immunoprecipitated proteins were eluted from the beads with sample buffer for 1h at room temperature and then electrophoretically separated on 7% (w/v) polyacrylamide gels. Gels were pre-fixed in methanol/acetic acid (30:10, v/v), washed in water and, for fluorography, soaked in 1M sodium salicylate for 60 min. After drying at 80°C for 2h, gels were exposed to X-ray films and further analysed and quantified by densitometry.

Iodide efflux

CFTR-mediated iodide effluxes were measured at room temperature using the cAMP agonist forskolin (Fsk 10µM) and the CFTR potentiator genistein (Gen, 50µM) or VX-770 (10µM) and Gen (50µM).

Biochemical determination of the plasma membrane levels of CFTR

To determine plasma membrane levels of CFTR protein, we performed cell surface biotinylation in BHK cells cultured on permeable growth supports or tissue culture plates using cell membrane impermeable EZ-Link™ Sulfo-NHS-SS-Biotin, followed by cell lysis in buffer containing 25 mM HEPES, pH 8.0, 1% (v/v) Triton, 10% glycerol (v/v), and Complete Protease Inhibitor Mixture, as described previously [23,24]. Biotinylated proteins were isolated by streptavidin-agarose beads, eluted into SDS-sample buffer, and separated by 7.5% (w/v) SDS-PAGE.

Multiple sequence alignment

Sequences for NBD domains of ABC transporters were obtained from Uniprot [25] (human and mouse CFTR) or the PDB [26] (1B0U, 1L2T, 1G29, 1G6H, 1JJ7). Alignments were performed with Jalview [27] using the T-Coffee [28] algorithm using the default parameters.

Data and Statistical analyses

The data and statistical analyses used in this study comply with the recommendations on experimental design and data analysis in pharmacology (Curtis et al., 2015). Quantitative results are shown as mean±SEM of *n* observations. To compare two sets of data, Student t-test was used and differences considered to be significant for *p-values* ≤ 0.05. In Western blotting (Figures 1-3), pulse chase (Figures 4, S3); cell surface biotinylation (Figure 4) and in iodide efflux studies (Table 1, Figure

#

5, S4 and S5), n represents the number of experiments performed with distinct cell cultures on different days, being thus biological replicates.

Reagents

All reagents used here were of the highest purity grade available. Forskolin and genistein were from Sigma-Aldrich (St. Louis, MI, USA); VX-809 and VX-770 were acquired from Selleck Chemicals (Houston, TX, USA).

CFTR was detected with the mouse anti-CFTR monoclonal 596Ab, which recognizes a region of NBD2 (1204 – 1211) from CFFT-Cystic Fibrosis Foundation Therapeutics CFF Therapeutics (Cui et al., 2007) and calnexin with rabbit polyclonal anti-calnexin Ab SPA-860, from Stressgen Biotechnologies Corporation (Victoria, BC, Canada).

Other specific reagents included: X-ray films (Kodak, supplied by Sigma-Aldrich); Complete Protease Inhibitor Mixture from Roche Applied Science (Penzberg, Germany); EZ-Link™ Sulfo-NHS-SS-Biotin from Pierce Chemical Company (Rockford, IL, USA).

#

RESULTS

Removal of short regulatory extension (RE_S) alone or with regulatory insertion (RI) has no impact on F508del-CFTR processing

The impact of deleting RE_S – short RE (Δ^{654}Ser-Gly^{673}, Figure S1) was first assessed, either alone or together with RI in its short and long variants (ΔRI_S, ΔRI_L), on the *in vivo* processing of wt- and F508del-CFTR by Western blot (WB) of BHK cells stably expressing such variants (Fig.1A,D,E; Table1). Removal of RE_S had no impact on processing of either F508del-CFTR or wt-CFTR (Fig.1A, lanes 5,10; Table1), despite that the immature form of ΔRE_S-F508del-CFTR appeared consistently at increased levels vs. those of F508del-CFTR (Fig.1A, lanes 5,2).

TABLE 1. Summary of Western blot quantification of original data in Fig.1-3 for different CFTR variants in the presence of VX-809 or DMSO control. Data are expressed as normalized ratios ((band C / band (B+C)) for each variant and as a percentage to wt-CFTR ratio.

		wt-background		F508del-background	
		Control	VX-809	Control	VX-809
	CFTR variant	% to wt	% to wt	% to wt	% to wt
	-	100 ± 1	103 ± 1	8 ± 1	17 ± 2
ΔRE_S	-	98 ± 2	100 ± 1	3 ± 2	9 ± 4
	ΔRI_S	54 ± 9	93 ± 3	7 ± 2	20 ± 4
	ΔRI_L	100 ± 1	97 ± 2	71 ± 3	96 ± 2
	R1070W	71 ± 6	90 ± 3	33 ± 7	26 ± 6
	G550E	101 ± 1	102 ± 1	37 ± 5	39 ± 4
ΔRE_L	-	88 ± 5	87 ± 3	9 ± 2	8 ± 2
	ΔH9	55 ± 3	69 ± 3	0 ± 0	0 ± 0
ΔH9		72 ± 4	69 ± 3	1 ± 0	0 ± 0
ΔRI_S	-	44 ± 2	90 ± 3	3 ± 2	4 ± 3
	R1070W	11 ± 3	56 ± 8	2 ± 0	4 ± 2
	G550E	82 ± 3	98 ± 1	6 ± 4	5 ± 3
ΔRI_L	-	101 ± 1	101 ± 0	78 ± 5	92 ± 4
	R1070W	92 ± 2	94 ± 3	96 ± 2	96 ± 3
	G550E	97 ± 2	92 ± 2	92 ± 4	97 ± 2
R1070W		69 ± 7	93 ± 4	34 ± 3	46 ± 4
G550E		101 ± 1	101 ± 1	42 ± 4	73 ± 6

Removal of RE_S together with RI_L – long RI (Δ^{404}Gly-Leu^{435}, Figure S1) led to a maturation increase of F508del-CFTR from 3±2% to 71±3% (vs wt-CFTR levels), similarly to what had been previously reported by Alexandrov *et al* for ΔRI_L alone [13]. In contrast, removal of RI_S – short RI (Δ^{412}Ala-Leu^{428}, Figure S1) had no impact on ΔRE_S-F508del-CFTR processing (Fig.1A, lanes 6,7; Fig.1E; Table1). So in summary, removal of RE_S jointly with RI_S or RI_L had no effect on F508del-CFTR processing.

Interestingly, when RE_S and RI_S, were jointly removed from wt-CFTR, its processing was significantly reduced to 54±9%, while ΔRE_S jointly with ΔRI_L caused no impact (Fig.1A, lanes11,12, respectively; Fig.1D; Table1). Again, these data were equivalent to removal of ΔRI_S or ΔRI_L alone on wt-CFTR processing (Fig.1A, lanes8,9; Fig.1E; Table1).

#

The differential effect caused by removal of RI_S vs RI_L on F508del- and wt-CFTR emphasize the importance of those 8 N-term (^{404}Gly-Ala^{412}) and 7 C-term (Leu^{428}-Leu^{435}) amino acid residues that differ between those 2 RI regions for the folding and processing of CFTR.

Simultaneous removal of long regulatory extension (RE_L) and helix H9 significantly reduces wt-CFTR processing but increases levels of F508del-CFTR immature form

Next, we assessed the impact of removing the long version of RE – RE_L (Δ^{647}Cys-Ser^{678}, Fig.2), which significantly decreased wt-CFTR processing to 88±5% (Fig.2A, lane 3; Fig.2C) but had no impact on F508del-CFTR (Fig.2A, lane4; Fig.2C). As helix H9 (Δ^{637}Gln-Gly^{646}, Figure S1) can be considered to be part of this longer RE region [22] since it interacts with RE (Figure S2), we also tested the effect of removing helix H9 jointly with ΔRE_L. Deletion of both H9 (ΔH9) and RE_L further decreased the residual processing of ΔRE_L-F508del-CFTR from 9±2 to 0±0% and in fact the same happened for ΔH9 alone (Fig.2a, lanes 8,6, respectively). Curiously, however, levels of immature F508del-CFTR were significantly increased when both RE_L and H9 were removed (Fig.2A, lane8), similarly to ΔRE_S-F508del-CFTR (Fig.1A) and in contrast to ΔRE_L-F508del-CFTR.

For wt-CFTR, ΔRE_L-ΔH9 also led to a decrease in processing (55±3%), which was more pronounced than for ΔRE_L alone, but interestingly removal of H9 helix alone only reduced processing to 72±4% (Fig.2A, lanes 7,5, respectively).

ΔRI_S, but not ΔRE_S, abolishes the plasma membrane rescue of F508del-CFTR by revertants

In order to test whether the stabilized immature form of ΔRE_S-F508del-CFTR could be rescued to mature form, we next tested the effects of removing the RE_S from F508del-CFTR with R1070W and G550E revertants. Indeed, both the R1070W and G550E revertants rescued ΔRE_S-F508del-CFTR to 33±7% and 37±5%, respectively (Fig.1C, lanes 6,10; Table1).

However, removal of RI_S from F508del-CFTR with R1070W and G550E revertants, virtually abolished the rescue of F508del-CFTR by both revertants (Fig.1C, lanes 4,8; Table1). Moreover, processing of ΔRI_L-F508del-CFTR was further increased by either R1070W or G550E up to 96±2% and 92±4%, respectively (Fig.1C, lanes 5,9; Table1). Alone, R1070W and G550E rescued F508del-CFTR from 8±1% to 34±3% and 42±4% respectively (Fig.1C, lanes 3,7; Table1), as we previously reported [5].

Interestingly, the impaired processing of ΔRI_S-wt-CFTR (44±2%) was significantly rescued by G550E (to 82±3%), but curiously it was further reduced by R1070W (to 11%) i.e., close to levels of F508del-CFTR processing (Fig.1B, lanes8,4; Table1). Of note that R1070W alone also reduced wt-CFTR

#

processing to 69±7%, but this reduction could be compensated by the removal of RI_L (92±2%) (Fig.1B, lanes 3,5; Table1), while G550E alone caused no effect on wt-CFTR processing (Fig.1B, lane7).

ΔRI_L synergises with VX-809, but not with revertants to rescue ΔRE_S-F508del-CFTR processing

To further test how the stabilized immature form of ΔRE_S-F508del-CFTR could be pharmacologically rescued, we then assessed the impact of corrector VX-809 (which *per se* promotes maturation of the F508del-CFTR) on the processing of this and of the other variants, to obtain structural insight on the effects of this novel drug. Although ΔRE_S-F508del-CFTR could not be rescued by VX-809, data show that this small molecule was able to rescue ΔRI_S-ΔRE_S-F508del-CFTR (from 7±2% to 20±4%) and further increased processing of ΔRI_L-ΔRE_S-F508del-CFTR to wt-CFTR levels (from 71±3% to 96±2%) (Fig.3A, lanes 6,7; Fig.3E; Table1). These data suggest a strong synergistic effect between VX-809 and ΔRI_L (and with ΔRI_S, albeit to a lesser extent) to rescue ΔRE_S-F508del-CFTR processing. This is particularly interesting because VX-809 did not rescue processing of the ΔRE_S-, nor ΔRI_S-F508del-CFTR variants (Fig.3A, lanes 5,3; Table1) while it recovered the processing of ΔRI_L-F508del-CFTR to wt-CFTR levels (Fig.3A, lane4; Table1). Notably, VX-809 was able to almost completely revert processing impairment of ΔRI_S-wt-CFTR and ΔRI_S-ΔRE_S-CFTR (from 44±2% and 54±9%) to 90±3% and 93±3%, respectively (Fig.3A, lanes8,11; Fig.3D; Table1).

Strikingly, VX-809 had no effect on processing of ΔRE_S-F508del-CFTR with R1070W or G550E (Fig.3C, lanes 6,10; Fig.3E; Table1), while it further rescued processing of F508del-CFTR variants with R1070W or G550E alone to 46±4% and 73±6%, respectively (Fig.3C, lanes 3,7; Fig.3E; Table 1), as reported [5]. Similarly, VX-809 caused no significant further rescue on the processing of ΔRI_L-F508del-CFTR with those revertants, but these variants already had processing levels close to those of wt-CFTR (Fig.3C, lanes 5, 9; Fig.3E; Table 1). Interestingly, the impaired processing of ΔRE_S-R1070W-wt-CFTR (71±6%) was also reverted by VX-809 to 90±3% (Fig.3B, lane 6; Table 1).

Corrector VX-809 failed to rescue any of the ΔRE_L-, ΔH9- and ΔRE_L-ΔH9-F508del-CFTR variants (Fig.2B, C), while significantly increasing the processing of the ΔRE_L-ΔH9-wt-CFTR from 55±3% to 69±3% (Fig.2B, lane 7; Fig.2C).

ΔRI_L-ΔRE_S-F508del-CFTR levels at the plasma membrane are equivalent to those of wt-CFTR

#

To determine the fraction of the above CFTR variants that localize to the PM, we used quantitative cell surface biotinylation. These data showed that PM levels of ΔRI_L-ΔRE_S-F508del-CFTR were equivalent to those of wt-CFTR, while those of ΔRI_L-F508del-CFTR were significantly lower (Fig.4A, lanes 5, 4; Fig.4B). Data also confirmed that ΔRE_S did not induce appearance of F508del-CFTR at the cell surface (data not shown). Corrector VX-809 further increased the PM expression of ΔRI_L-ΔRE_S-F508del-CFTR to levels that are significantly higher than those of wt-CFTR (Fig.4A, lanes 2, 9, Fig.4B). This compound also significantly increased PM levels of ΔRI_L-F508del-CFTR to similar levels of wt-CFTR (Fig.4A, lanes 2, 8; Fig.4B).

Given the very significant stabilization of immature ΔRE_S-F508del-CFTR (Fig.1A), next, we determined how removal of ΔRE_S affected the processing efficiency and the turnover of the F508del- and ΔRI_L-F508del-CFTR variants. To this end, we performed pulse-chase experiments (Fig.4C, D) and indeed our results revealed that ΔRE_S very significantly stabilized immature F508del-CFTR not just relatively to F508del-CFTR but to levels even significantly higher than those of wt-CFTR (Fig.4C, D). Interestingly, this stabilizing effect was no longer significant for ΔRI_L-ΔRE_S-F508del-CFTR nor for ΔRI_L-F508del-CFTR, the latter being equivalent to wt-CFTR (Fig.4C, D). Removal of RI_S from F508del-CFTR did not stabilize its turnover (data not shown). As to removal of either RE_S or RI_S from wt-CFTR, it did not affect the processing efficiency or the turnover vs wt-CFTR (Figure S3).

VX-809 jointly with RE and RI removal completely restored F508del-CFTR function as chloride channel

To investigate the channel function of the ΔRE_S- and ΔRI_L-F508del-CFTR variants, we used the iodide efflux technique. Removal of RE_S alone had no impact on F508del-CFTR function (Fig.5A; black dash line in Figure S4B) as expected from the lack of processed form for this variant (Fig.1A). However, when RE_S and RI_L were removed jointly from F508del-CFTR, functional levels reached 78±7% of wt-CFTR (Fig.5A, C; black dotted line in Figure S4B). As to removal of RI_L alone from F508del-CFTR, it restored function to 92±7% of wt-CFTR (Fig.5A, C; black line in Figure S4B), as described [13]. Also, the delay in peak response observed for F508del-CFTR (min=4) vs wt-CFTR (min=2), was partially corrected (to min=3) both by removal of RI_L alone from F508del-CFTR or together with RE_S (Fig.5C; Figure S4B, black line and dotted line).

Introduction of G550E and R1070W revertants into the ΔRI_L-F508del-CFTR variant slightly but not significantly decreased its function from 92±7% to 71±8% and 76±8%, respectively (Fig.5A, C; black lines in Figure S4C, D), in parallel to the respective processing levels (Fig.1). In fact, these variants showed higher activity levels than the revertants containing RI_L (29±3% and 56±6%, respectively).

#

Interestingly however, both G550E- and R1070W-ΔRI$_L$-F508del-CFTR fully corrected (to min=2) the delay in peak response of F508del-CFTR, which was still partially present in ΔRI$_L$- and ΔRI$_L$-RE$_S$-F508del-CFTR (min=3).

The effect of VX-809 (3μM, 48h at 37ºC) was also examined at functional level on the ΔRE$_S$-, ΔRI$_L$-ΔRE$_S$- and ΔRI$_L$-F508del-CFTR variants. Strikingly VX-809 caused an increase in ΔRE$_S$-ΔRI$_L$-F508del-CFTR function (84±8% of wt-CFTR) which was parallel to the observed increase in PM expression (Fig.4; Fig.5A, C; black dotted line in Figure S4F). Also, ΔRE$_S$-ΔRI$_L$-F508del-CFTR fully corrected (to min=2) the delay in peak response of F508del-CFTR which was still partially present in ΔRI$_L$- and ΔRI$_L$-ΔRE$_S$-F508del-CFTR (min=3).

In contrast to the observed increase in processing, VX-809 caused no significant increase in the function of ΔRI$_L$-F508del-CFTR and actually a slight, but not significant decrease was observed and there was still the same delay in peak response (Fig.5A, C; black line in Figure S4F).

A similar slight decrease in function was observed for VX-809 on the ΔRI$_L$-R1070W-F508del-CFTR variant (Fig.5A, C; black line in Figure S4H), but the most striking result was observed for the significant decrease caused by VX-809 on function of ΔRI$_L$-G550E-F508del from 76±8 to 41±3% (Fig.5A, C; black line in Figure S4G). Nevertheless both revertant variants of ΔRI$_L$-F508del-CFTR showed no change in peak response which was still the same as wt-CFTR (min=2).

VX-770-stimulated currents of CFTR variants are dramatically decreased by ΔRI$_L$ but not by ΔRI$_L$-ΔRE$_S$

Given the interesting and diverse results observed for the ΔRE$_S$ and ΔRI$_L$ under VX-809, next we tested the effects of potentiator VX-770 (Ivacaftor), an approved drug for CF patients with gating mutations (Fig.5B) on these variants and in combination with VX-809, for F508del/F508del patents. Most strikingly, our data show that VX-770/Fsk significantly decreased the function of ΔRI$_L$-F508del-CFTR *vs* potentiation by Gen/Fsk (Fig.5B, C) from 92±7% to 58±7% of wt-CFTR (Fig.5B, C; black line in Figure S4J). As ΔRE$_S$-F508del-CFTR was not processed, we did not test the effect of VX-770 on this variant, but when the ΔRE$_S$-ΔRI$_L$-F508del-CFTR variant was assessed for its function after acute application of VX-770 with Fsk, an increase in function (to 87±3% of wt-CFTR) was observed vs its function under Gen/Fsk (78±7% of wt-CFTR) (Fig.5B, C; black dotted line in Figure S4J).

The most dramatic result, however, was observed for the ΔRI$_L$-G550E-F508del-CFTR variant which under VX-770/Fsk only had 4±1% function of wt-CFTR, while under Gen/Fsk it had 76±8% (Fig.5B, C; black line in Figure S4K). For ΔRI$_L$-R1070W-F508del-CFTR this decrease was not observed (Fig.5B, C;

#

black line in Figure S4L), and in fact this variant had a slightly higher function under VX-770 stimulation (72±4%) than ΔRI_L-F508del-CFTR (58±7%) (Fig.5B, C, black line in Figure S4H).

The delay in peak response of F508del- vs. wt-CFTR was not corrected for ΔRI_L-F508del-CFTR (min=3), but it was corrected for ΔRI_L-ΔRE_S-F508del-CFTR (min=2) (black and dotted black lines in Figure S4J, respectively). Curiously, on the other hand ΔRI_L-R1070W-F508del-CFTR showed the quickest peak response (at min=1), in contrast to either R1070W-F508del-CFTR or ΔRI_L-F508del-CFTR, both at min=3.

Similarly, VX-770 also significantly decreased the function of ΔRI_L-wt-CFTR from 127±15% under Gen to 57±6% (Figure S5).

#

Discussion

The main goal of this study was to understand how the removal of the regulatory extension (ΔRE) alone or with the regulatory insertion (ΔRI)- two highly conformationally dynamic regions - impacted on the rescue of F508del-CFTR processing and function by two compounds - VX-809 and VX-770 - which in combination were recently approved o clinically treat F508del-homozygous patients. Indeed, CFTR is the sole ABC that functions as a channel and thus, these highly dynamic RE and RI regions which are absent in other ABC transporters, may be of high relevance to understand how CFTR differs from other ABCs, namely in its function as a channel.

These regions RE and RI were originally suggested to be positioned to impede formation of the NBD1-NBD2 dimer required for channel gating [16,17]. Indeed, both RI and RE were shown to be mobile elements in solution that bind transiently to the core of NBD in the ß-sheet and α/ß subdomains of NBD1[3]. Similarly to what demonstrated for RI[13], is plausible to posit that the dynamic flexibility of the RE may also result in exposure of hydrophobic surfaces thus contributing to the dynamic instability of NBD1 and thus contribute to the low folding efficiency of F508del-CFTR. The RE is a ~30-residue segment at NBD1 C-terminus, so-called because it goes beyond canonical ABC NBDs [16]. Although this region was absent from the solved CFTR- NBD1 crystal structure [17], it was described as a helix packing against NBD1 at the NBD1:NBD2 interface and NMR data showed it has significant conformational flexibility [3,20]. Notwithstanding, there is some controversy regarding the RE boundaries. The RE (previously called H9c) was defined as ^{655}Ala-Ser^{670} [16,17], ^{639}Asp-Ser^{670} [21] or ^{654}Ser-Gly^{673} [3]. According to the crystal structure (PDB code 2PZE), NBD1 extends only to ^{646}Gly, where RD begins, so RE could be proposed to start at ^{647}Cys [3,22], being thus considered as part of RD, a domain absent in other ABC transporters [1]. As for the RI (previously called S1-S2 loop) its limits are also variable, being firstly described as a ~35-residue segment (^{405}Phe-^{436}Leu) consisting of α-helices H1b and H1c [16] (Fig.S1). Later, however, these limits were proposed to be ^{404}Gly-Leu^{435} [13,21] or ^{405}Phe-Leu^{436} [22].

Impact of RE and RI on CFTR processing and function

Our data shown here on CFTR variants depleted of different versions of the RE dynamic region demonstrate that unlike RI deletion, removal of short RE - ΔRE_S (Δ^{654}Ser-Gly^{673}) did not *per se* rescue F508del-CFTR processing. Nevertheless, ΔRE_S dramatically stabilized the immature form of F508del-CFTR (see Fig.6). In fact, our pulse-chase experiments show that the immature form of ΔRE_S-F508del-CFTR exhibits a turnover rate which is ~2.7 fold lower than that of wt-CFTR. Of note, when Aleksandrov *et al* removed the dynamic region RI from F508del-CFTR they found a dramatic increase

#

in the channel thermostability, even augmented for higher temperatures [13]. Interestingly however, removal of the RE_S from ΔRI_L-F508del-CFTR (ΔRI_L: Δ^{404}Gly-Leu^{435}) while not affect processing, it further reduced its function (from 92% to 78%).

The latter findings on function of ΔRE_S-wt-CFTR and ΔRE_S-ΔRI_L-F508del-CFTR were somewhat surprising since the RE was previously described to impede putative NBD1:NBD2 dimerization that is required for channel gating [21]. Accordingly, an increase in CFTR activity would be expected upon ΔRE_S removal, which is actually the opposite of what we observe for wt-CFTR. Besides the fact that those authors studied a different RE version (^{639}Asp-Ser^{670}), this discrepancy could derive from structural constraints and lack of flexibility of the 'single polypeptide' protein that we used, vs their 'split' CFTR channels (2 'halves' of 633 and 668 aa) for which channel function was indistinguishable from wt-CFTR [21]. Moreover, since RD phosphorylation is required for channel gating [29,30], the reduced function of ΔRE_S-wt-CFTR may also result from absence of ^{660}Ser and ^{670}Ser [19,20]. Although the RD contains more than ten PKA phospho-sites and no individual one is essential, phosphorylation of increasing numbers of sites enables progressively greater channel activity [31].

Removal of a longer RE version (ΔRE_L: Δ^{647}Cys-Ser^{678}) was without effect on F508del-CFTR processing and significantly reduced that of wt-CFTR to 88%. Such differential impact on wt- and F508del-CFTR is consistent with the conformational heterogeneity between these two proteins lacking both RI and RE [32].

Removal of RI short version, RI_s (Δ^{412}Ala-Leu^{428}) significantly reduced wt-CFTR processing to less than half of its normal levels, while not rescuing F508del-CFTR processing, thus being essential for CFTR proper folding. This is in contrast to removal of long RI (ΔRI_L) which led to 78% processing F508del-CFTR, as reported [13] but without impact on wt-CFTR. These data indicate that those 8/ 7 amino acid residues at the N-term/ C-term of RI_S (and absent in RI_L) impair the folding efficiency and processing of both wt- and F508del-CFTR.

The recently published cryo-EM structure of human CFTR [33] indicates that these regions are structurally disordered. Consistently, the RI loop in NBD1 is described in the of zebrafish CFTR cryo-structure to contribute to the amorphous density that is observed between NBD1 and the elbow helix of TMD2 [34]. From a structural point of view, models of the full-length CFTR protein suggest that the two regions (RI and RE) behave differently. The distances between the extremities of the deleted parts are indeed different (ΔRI_S = 18Å, ΔRI_L= 10Å versus ΔRE_S = 27Å, ΔRE_L = 30Å). The longer distances observed for ΔRE imply a substantial reorganization of the C-terminal parts of NBD1 and NBD2, which precludes a clear understanding of what might happen upon these deletions. In contrast, the lower distances observed for ΔRI (near a possible minimum of 6Å) allows a better simulation of the

possible structural behaviour of these constructs. Indeed, preliminary molecular dynamics simulations of the ΔRI_L-F508del-CFTR suggested that in this case, part of the RD is reorganized and partially takes space left by the ΔRI deletion, thereby substituting it for tight contacts with NBD2. Meanwhile, following a probable allosteric effect [13,22,35], contact of NBD1-F508 with ICL4 residue L1077 (a likely essential contact for channel opening), is nearly completely restored by I507. Such a feature is not observed in the F508del-CFTR model (B. Hoffmann, I. Callebaut and J.-P. Mornon, personal communication).

Effect of VX-809 on F508del-CFTR variants lacking RE and RI

As for rescue of CFTR variants lacking RE and RI by CFTR modulators, VX-809 restored the processing of both ΔRE_S-ΔRI_L- and ΔRI_L-F508del-CFTR variants equally well and to wt-CFTR levels (from 71-78% to 92-96%. These data suggest a strong synergistic effect between VX-809 and ΔRI_L to rescue ΔRE_S-F508del-CFTR processing and thus some possible interference of the regulatory insertion with VX-809 binding to F508del-CFTR (see Fig.6). Indeed, although previous studies [5,36,37] suggested putative binding of VX-809 to NBD1:MSD2 (ICL4) interface (see Fig.6), they also suggested scope for further F508del-CFTR correction at distinct conformational sites, so data shown here suggest that VX-809 may also bind to the regulatory insertion.

Interestingly, the processing defect of ΔRI_S-wt-CFTR (but not of ΔRI_S-F508del-CFTR) was rescuable by VX-809 to 90%, indicating that the amino acid stretches of the RI_L that remain present in RI_S do not affect the rescue of ΔRI_S-wt-CFTR but preclude rescue of F508del-CFTR by VX-809.

We also tested here the impact of removing helix 9 (H9) which precedes the RE (^{635}Gln-Gly^{646}), just after H8 (^{630}Phe-Leu^{634}), both helices proposed to interact with the NBD1:NBD2 heterodimer interface by folding onto the NBD1 ß-subdomain [20,32] as well as to bind ICL4 near Phe508. When H9 is present, ΔRE_L-wt-CFTR processing appears to be favoured by VX-809, suggesting some synergy of this small molecule with H9 helix to correct the conformational defect(s) caused by ΔRE_L on wt-CFTR. These data are in contrast to ΔH9-F508del-CFTR which exhibits 0% processing with or without ΔRE_L and no rescue by VX-809.

Very strikingly, and in contrast to its effect on processing, was the effect of ΔRI_L on the VX-770 stimulated currents which were decreased by almost half vs those stimulated by Gen/Fsk (92% to 58%). These data seem to indicate that the absence of the regulatory insertion could impair (and its presence favour) binding of VX-770 to CFTR (see Fig.6). Surprisingly, the removal of RE_s from ΔRI_L-F508del-CFTR could correct this defect and restore the maximal function by VX-770 (see Fig.6). Indeed, under VX-770, ΔRE_S-ΔRI_L-F508del-CFTR exhibited significantly higher activity (87%) than ΔRI_L-

#

F508del-CFTR (58%). In contrast, removal of RE_S from wt-CFTR significantly reduced its function *vs* that of wt-CFTR (down to 70%) but had no effect on processing.

Impact of F508del-revertants on CFTR variants lacking RE and RI

Another goal of the present study was to assess how presence of the F508del-CFTR revertants G550E and R1070W [5,10,11] influence variants without RE and RI. Remarkably, our data show that the presence of either of these revertants did not affect ΔRE_S-F508del-CFTR processing, but both of them further increased processing (but not function) of ΔRI_L-F508del-CFTR to almost levels of wt-CFTR: 92-96% (G550E) and 71-76% (R1070W).

In contrast, removal of RI_S from either of these F508del-CFTR revertants completely abolished their processing, emphasizing how important the different residues between RI_S and RI_L are for F508del-CFTR conformers partially rescued by the revertants.

Regarding wt-CFTR processing, G550E (at the NBD1:NBD2 dimer interface) also partially recovered the negative effect caused by RI_S removal. In contrast, R1070W (at the NBD1:ICL4 interface), negatively affected processing of wt-CFTR (to 69%) and of ΔRI_S-wt-CFTR (from 44% to 11%), while not affecting ΔRI_L-wt-CFTR. R1070W rescues F508del-CFTR because Trp1070 fills the gap created by deletion of residue Phe508 [38]. It is not surprising that it perturbs CFTR folding due to clashing of ^{508}Phe and ^{1070}Trp residues. It is, nevertheless curious that R1070W affect more the processing ΔRI_S-wt-CFTR than wt-CFTR, to levels of F508del-CFTR, suggesting that both changes affect the same region of the molecule. Rescue of both R1070W-wt-CFTR and R1070W-ΔRI_S-wt-CFTR by VX-809 further supports this concept.

The most striking effect of ΔRI_L however, was the almost complete abolition of VX-770-stimulated current of G550E-F508del-CFTR to levels even lower than those observed for ΔRI_L-F508del-CFTR (see above). It was suggested that VX-770 binds directly to CFTR to the MSDs (although it is not defined the exact binding site), in phosphorylation-dependent but ATP-independent manner and away from the canonical catalytic site [39,40]. Both RD and RI were suggested by Eckford and colleagues as putative binding regions for VX-770 [39]. Nevertheless, the pharmacological effect of VX-770 remains robust in the absence of the RD [40] and here we demonstrate that it does indeed require RI since VX-770 is unable to stimulate either ΔRI_L-F508del-CFTR or ΔRI_L-G550E- F508del-CFTR (see Fig.6).

Overall, our data show that while the presence of the regulatory insertion seems to be precluding full rescue of F508del-CFTR processing by VX-809, this region appears essential to rescue its function

by VX-770, thus suggesting some contradictory role in rescue of F508del-CFTR by these two modulators. Nevertheless, this negative impact of RI_L removal on VX-770-stimulated currents on F508del-CFTR can be compensated by deletion of the regulatory extension which also leads to the stabilization of this mutant. We thus propose that, despite both these regions being conformationally active, RI precludes F508del-CFTR processing while RE affects mostly its stability and channel opening.

#

Acknowledgements: Work supported by grants PTDC/SAU-GMG/122299/2010 (to MDA) and UID/MULTI/04046/2013 centre grant (to BioISI), both from FCT/MCTES/PIDDAC, Portugal. IU, ACDP and VF are/were recipients of SFRH/BD/69180/2010, SFRH/BD/17475/2004, SFRH/BD/87478/2012 PhD fellowships and HMB of SFRH/BPD/93017/2013 post-doctoral fellowship (FCT, Portugal), respectively. Authors acknowledge I Callebaut, B Hoffmann and J-P Mornon for the revision of the manuscript and for the helpful comments.

Conflict of interest: The authors declare no conflict of interest related to this paper.

Author Contributions: IU, ACDP, SA, MJL, VF and CMF preformed the experiments; MDA designed the study and obtained funding; IU, ACDP, HB and MDA interpreted the data, wrote the manuscript.

#

REFERENCES

(1) Riordan, J. R. (2008) CFTR function and prospects for therapy. *Annu. Rev. Biochem. 77*, 701–726.
(2) Sheppard, D. N., and Welsh, M. J. (1999) Structure and function of the CFTR chloride channel. *Physiol. Rev. 79*, S23–45.
(3) Kanelis, V., Hudson, R. P., Thibodeau, P. H., Thomas, P. J., and Forman-Kay, J. D. (2010) NMR evidence for differential phosphorylation-dependent interactions in WT and DeltaF508 CFTR. *EMBO J. 29*, 263–277.
(4) Serohijos, A. W. R., Hegedus, T., Aleksandrov, A. A., He, L., Cui, L., Dokholyan, N. V., and Riordan, J. R. (2008) Phenylalanine-508 mediates a cytoplasmic-membrane domain contact in the CFTR 3D structure crucial to assembly and channel function. *Proc. Natl. Acad. Sci. U. S. A. 105*, 3256–3261.
(5) Farinha, C. M., King-Underwood, J., Sousa, M., Correia, A. R., Henriques, B. J., Roxo-Rosa, M., Da Paula, A. C., Williams, J., Hirst, S., Gomes, C. M., and Amaral, M. D. (2013) Revertants, low temperature, and correctors reveal the mechanism of F508del-CFTR rescue by VX-809 and suggest multiple agents for full correction. *Chem. Biol. 20*, 943–955.
(6) He, L., Aleksandrov, A. A., Serohijos, A. W. R., Hegedus, T., Aleksandrov, L. A., Cui, L., Dokholyan, N. V., and Riordan, J. R. (2008) Multiple membrane-cytoplasmic domain contacts in the cystic fibrosis transmembrane conductance regulator (CFTR) mediate regulation of channel gating. *J. Biol. Chem. 283*, 26383–26390.
(7) Denning, G. M., Anderson, M. P., Amara, J. F., Marshall, J., Smith, A. E., and Welsh, M. J. (1992) Processing of mutant cystic fibrosis transmembrane conductance regulator is temperature-sensitive. *Nature 358*, 761–764.
(8) Teem, J. L., Berger, H. A., Ostedgaard, L. S., Rich, D. P., Tsui, L. C., and Welsh, M. J. (1993) Identification of revertants for the cystic fibrosis delta F508 mutation using STE6-CFTR chimeras in yeast. *Cell 73*, 335–346.
(9) Teem, J. L., Carson, M. R., and Welsh, M. J. (1996) Mutation of R555 in CFTR-delta F508 enhances function and partially corrects defective processing. *Receptors Channels 4*, 63–72.
(10) DeCarvalho, A. C. V., Gansheroff, L. J., and Teem, J. L. (2002) Mutations in the nucleotide binding domain 1 signature motif region rescue processing and functional defects of cystic fibrosis transmembrane conductance regulator delta f508. *J. Biol. Chem. 277*, 35896–35905.
(11) Roxo-Rosa, M., Xu, Z., Schmidt, A., Neto, M., Cai, Z., Soares, C. M., Sheppard, D. N., and Amaral, M. D. (2006) Revertant mutants G550E and 4RK rescue cystic fibrosis mutants in the first nucleotide-binding domain of CFTR by different mechanisms. *Proc. Natl. Acad. Sci. U. S. A. 103*, 17891–17896.
(12) Loo, T. W., Bartlett, M. C., and Clarke, D. M. (2010) The V510D suppressor mutation stabilizes DeltaF508-CFTR at the cell surface. *Biochemistry (Mosc.) 49*, 6352–6357.

#

(13) Aleksandrov, A. A., Kota, P., Aleksandrov, L. A., He, L., Jensen, T., Cui, L., Gentzsch, M., Dokholyan, N. V., and Riordan, J. R. (2010) Regulatory insertion removal restores maturation, stability and function of DeltaF508 CFTR. *J. Mol. Biol. 401*, 194–210.

(14) Van Goor, F., Hadida, S., Grootenhuis, P. D. J., Burton, B., Stack, J. H., Straley, K. S., Decker, C. J., Miller, M., McCartney, J., Olson, E. R., Wine, J. J., Frizzell, R. A., Ashlock, M., and Negulescu, P. A. (2011) Correction of the F508del-CFTR protein processing defect in vitro by the investigational drug VX-809. *Proc. Natl. Acad. Sci. U. S. A. 108*, 18843–18848.

(15) Wainwright, C. E., Elborn, J. S., Ramsey, B. W., Marigowda, G., Huang, X., Cipolli, M., Colombo, C., Davies, J. C., De Boeck, K., Flume, P. A., Konstan, M. W., McColley, S. A., McCoy, K., McKone, E. F., Munck, A., Ratjen, F., Rowe, S. M., Waltz, D., Boyle, M. P., TRAFFIC Study Group, and TRANSPORT Study Group. (2015) Lumacaftor-Ivacaftor in Patients with Cystic Fibrosis Homozygous for Phe508del CFTR. *N. Engl. J. Med. 373*, 220–231.

(16) Lewis, H. A., Buchanan, S. G., Burley, S. K., Conners, K., Dickey, M., Dorwart, M., Fowler, R., Gao, X., Guggino, W. B., Hendrickson, W. A., Hunt, J. F., Kearins, M. C., Lorimer, D., Maloney, P. C., Post, K. W., Rajashankar, K. R., Rutter, M. E., Sauder, J. M., Shriver, S., Thibodeau, P. H., Thomas, P. J., Zhang, M., Zhao, X., and Emtage, S. (2004) Structure of nucleotide-binding domain 1 of the cystic fibrosis transmembrane conductance regulator. *EMBO J. 23*, 282–293.

(17) Lewis, H. A., Zhao, X., Wang, C., Sauder, J. M., Rooney, I., Noland, B. W., Lorimer, D., Kearins, M. C., Conners, K., Condon, B., Maloney, P. C., Guggino, W. B., Hunt, J. F., and Emtage, S. (2005) Impact of the deltaF508 mutation in first nucleotide-binding domain of human cystic fibrosis transmembrane conductance regulator on domain folding and structure. *J. Biol. Chem. 280*, 1346–1353.

(18) Dahan, D., Evagelidis, A., Hanrahan, J. W., Hinkson, D. A., Jia, Y., Luo, J., and Zhu, T. (2001) Regulation of the CFTR channel by phosphorylation. *Pflüg. Arch. Eur. J. Physiol. 443 Suppl 1*, S92–96.

(19) Pasyk, S., Molinski, S., Ahmadi, S., Ramjeesingh, M., Huan, L.-J., Chin, S., Du, K., Yeger, H., Taylor, P., Moran, M. F., and Bear, C. E. (2015) The major cystic fibrosis causing mutation exhibits defective propensity for phosphorylation. *Proteomics 15*, 447–461.

(20) Bozoky, Z., Krzeminski, M., Muhandiram, R., Birtley, J. R., Al-Zahrani, A., Thomas, P. J., Frizzell, R. A., Ford, R. C., and Forman-Kay, J. D. (2013) Regulatory R region of the CFTR chloride channel is a dynamic integrator of phospho-dependent intra- and intermolecular interactions. *Proc. Natl. Acad. Sci. U. S. A. 110*, E4427–4436.

(21) Csanády, L., Chan, K. W., Nairn, A. C., and Gadsby, D. C. (2005) Functional roles of nonconserved structural segments in CFTR's NH2-terminal nucleotide binding domain. *J. Gen. Physiol. 125*, 43–55.

#

(22) Dawson, J. E., Farber, P. J., and Forman-Kay, J. D. (2013) Allosteric coupling between the intracellular coupling helix 4 and regulatory sites of the first nucleotide-binding domain of CFTR. *PloS One 8*, e74347.
(23) Moyer, B. D., Loffing, J., Schwiebert, E. M., Loffing-Cueni, D., Halpin, P. A., Karlson, K. H., Ismailov, I. I., Guggino, W. B., Langford, G. M., and Stanton, B. A. (1998) Membrane trafficking of the cystic fibrosis gene product, cystic fibrosis transmembrane conductance regulator, tagged with green fluorescent protein in madin-darby canine kidney cells. *J. Biol. Chem. 273*, 21759–21768.
(24) Swiatecka-Urban, A., Duhaime, M., Coutermarsh, B., Karlson, K. H., Collawn, J., Milewski, M., Cutting, G. R., Guggino, W. B., Langford, G., and Stanton, B. A. (2002) PDZ domain interaction controls the endocytic recycling of the cystic fibrosis transmembrane conductance regulator. *J. Biol. Chem. 277*, 40099–40105.
(25) UniProt Consortium. (2015) UniProt: a hub for protein information. *Nucleic Acids Res. 43*, D204–212.
(26) Berman, H. M., Westbrook, J., Feng, Z., Gilliland, G., Bhat, T. N., Weissig, H., Shindyalov, I. N., and Bourne, P. E. (2000) The Protein Data Bank. *Nucleic Acids Res. 28*, 235–242.
(27) Waterhouse, A. M., Procter, J. B., Martin, D. M. A., Clamp, M., and Barton, G. J. (2009) Jalview Version 2--a multiple sequence alignment editor and analysis workbench. *Bioinforma. Oxf. Engl. 25*, 1189–1191.
(28) Notredame, C., Higgins, D. G., and Heringa, J. (2000) T-Coffee: A novel method for fast and accurate multiple sequence alignment. *J. Mol. Biol. 302*, 205–217.
(29) Chappe, V., Irvine, T., Liao, J., Evagelidis, A., and Hanrahan, J. W. (2005) Phosphorylation of CFTR by PKA promotes binding of the regulatory domain. *EMBO J. 24*, 2730–2740.
(30) Mense, M., Vergani, P., White, D. M., Altberg, G., Nairn, A. C., and Gadsby, D. C. (2006) In vivo phosphorylation of CFTR promotes formation of a nucleotide-binding domain heterodimer. *EMBO J. 25*, 4728–4739.
(31) Hegedus, T., Serohijos, A. W. R., Dokholyan, N. V., He, L., and Riordan, J. R. (2008) Computational studies reveal phosphorylation-dependent changes in the unstructured R domain of CFTR. *J. Mol. Biol. 378*, 1052–1063.
(32) Hudson, R. P., Chong, P. A., Protasevich, I. I., Vernon, R., Noy, E., Bihler, H., An, J. L., Kalid, O., Sela-Culang, I., Mense, M., Senderowitz, H., Brouillette, C. G., and Forman-Kay, J. D. (2012) Conformational changes relevant to channel activity and folding within the first nucleotide binding domain of the cystic fibrosis transmembrane conductance regulator. *J. Biol. Chem. 287*, 28480–28494.

#

(33) Liu, F., Zhang, Z., Csanády, L., Gadsby, D. C., and Chen, J. (2017) Molecular Structure of the Human CFTR Ion Channel. *Cell 169*, 85–95.e8.
(34) Zhang, Z., and Chen, J. (2016) Atomic Structure of the Cystic Fibrosis Transmembrane Conductance Regulator. *Cell 167*, 1586–1597.e9.
(35) Aleksandrov, A. A., Kota, P., Cui, L., Jensen, T., Alekseev, A. E., Reyes, S., He, L., Gentzsch, M., Aleksandrov, L. A., Dokholyan, N. V., and Riordan, J. R. (2012) Allosteric modulation balances thermodynamic stability and restores function of ΔF508 CFTR. *J. Mol. Biol. 419*, 41–60.
(36) He, L., Kota, P., Aleksandrov, A. A., Cui, L., Jensen, T., Dokholyan, N. V., and Riordan, J. R. (2013) Correctors of ΔF508 CFTR restore global conformational maturation without thermally stabilizing the mutant protein. *FASEB J. Off. Publ. Fed. Am. Soc. Exp. Biol. 27*, 536–545.
(37) Okiyoneda, T., Veit, G., Dekkers, J. F., Bagdany, M., Soya, N., Xu, H., Roldan, A., Verkman, A. S., Kurth, M., Simon, A., Hegedus, T., Beekman, J. M., and Lukacs, G. L. (2013) Mechanism-based corrector combination restores ΔF508-CFTR folding and function. *Nat. Chem. Biol. 9*, 444–454.
(38) Thibodeau, P. H., Richardson, J. M., Wang, W., Millen, L., Watson, J., Mendoza, J. L., Du, K., Fischman, S., Senderowitz, H., Lukacs, G. L., Kirk, K., and Thomas, P. J. (2010) The cystic fibrosis-causing mutation deltaF508 affects multiple steps in cystic fibrosis transmembrane conductance regulator biogenesis. *J. Biol. Chem. 285*, 35825–35835.
(39) Eckford, P. D. W., Li, C., Ramjeesingh, M., and Bear, C. E. (2012) Cystic fibrosis transmembrane conductance regulator (CFTR) potentiator VX-770 (ivacaftor) opens the defective channel gate of mutant CFTR in a phosphorylation-dependent but ATP-independent manner. *J. Biol. Chem. 287*, 36639–36649.
(40) Jih, K.-Y., and Hwang, T.-C. (2013) Vx-770 potentiates CFTR function by promoting decoupling between the gating cycle and ATP hydrolysis cycle. *Proc. Natl. Acad. Sci. U. S. A. 110*, 4404–4409.
(41) Farinha, C. M., King-Underwood, J., Sousa, M., Correia, A. R., Henriques, B. J., Roxo-Rosa, M., Da Paula, A. C., Williams, J., Hirst, S., Gomes, C. M., and Amaral, M. D. (2013) Revertants, low temperature, and correctors reveal the mechanism of F508del-CFTR rescue by VX-809 and suggest multiple agents for full correction. *Chem. Biol. 20*, 943–955.
(42) Jih, K.-Y., and Hwang, T.-C. (2013) Vx-770 potentiates CFTR function by promoting decoupling between the gating cycle and ATP hydrolysis cycle. *Proc. Natl. Acad. Sci. U. S. A. 110*, 4404–4409.

#

FIGURE LEGENDS

FIGURE 1. Effect of removal of short regulatory extension (ΔRE_S) on processing of wt- and F508del-CFTR. (A–C) Samples from BHK cell lines stably expressing different CFTR variants of ΔRE_S and ΔRI, the latter either in its short "S" or long "L" versions (see Methods) and alone (A) or jointly with (B, C) genetic revertants, as indicated, were analysed for CFTR protein expression by WB with Ab anti-CFTR and also anti-calnexin (CNX) as loading control. All samples were incubated with 3μM DMSO for 48h, as controls for experiments with corrector VX-809 (see Fig.3). Summary of data of CFTR variants on the wt- (D) or F508del- (E) CFTR backgrounds, expressed as normalized ratios (band C/(band C+band B)) and as a percentage to the respective ratio for wt-CFTR and as mean ± standard error of the mean (SEM). (n) indicates nr. of independent experiments. "*" and "#" indicate significantly different ($p<0.05$) from wt-CFTR and F508del-CFTR, respectively.

FIGURE 2. Effect of removal of helix H9 in combination with ΔRE_L and VX-809 on processing of wt- and F508del-CFTR. (A, B) WB analysis of samples from BHK cell lines stably expressing wt- or F508del-CFTR variants with ΔRE_L, ΔH9 or ΔRE_L-ΔH9. Cells were incubated with 3μM VX-809 or DMSO (control) for 48h at 37ºC. CFTR protein expression was analysed by WB with the anti-CFTR and anti-CNX Abs. (C) Summary of data expressed as normalized ratios (Band C / (Band C+B)) and as a percentage to the respective ratios on the wt- or F508del-CFTR backgrounds and shown as mean±SEM. (n) indicates nº of independent experiments. "#" indicates significantly different from the respective variant treated with DMSO. "*" and "**" indicate significantly different from wt- or F508del-CFTR, respectively.

FIGURE 3. Effect of VX-809 on processing of wt- and F508del-CFTR variants without regulatory extension. (A-C) WB of samples from BHK cell lines stably expressing different CFTR variants of ΔRE and ΔRI, as indicated, alone (A) or jointly with (B, C) genetic revertants (see Methods). CFTR protein expression was analysed by WB with anti-CFTR and anti-CNX Abs as in Fig.1. All samples were incubated with 3μM VX-809 for 48h. (D, E) Summary of data of variants on the wt- (D) or F508del- (E) CFTR backgrounds, expressed as normalized ratios (band C/(band C+band B)) and as a percentage to the respective ratio for wt-CFTR and as mean±SEM. (n) indicates nº of independent experiments. "*" indicates significantly different ($p<0.05$) from respective variant without VX-809 (as shown in Fig.1 and indicated here by dashed bars).

#

FIGURE 4. Plasma membrane levels, efficiency of processing and turnover of immature CFTR without Regulatory Extension (RE_S). (A) BHK cells expressing ΔRI_L-F508del and ΔRI_L-ΔRE_S-F508del-CFTR and treated with 3μM VX-809 for 48h (or DMSO control) were subjected to cell surface biotinylation. wt-CFTR samples not treated with biotin were the negative control (NC). After streptavidin pull-down, CFTR was detected by WB. CFTR and CNX are detected in the whole cell lysate (WCL) as controls. (B) Quantification of data in (a) for PM CFTR normalized to total protein and shown as fold change relatively to wt-CFTR cells treated with DMSO. "*" and "#" indicate significantly different from wt-CFTR treated with DMSO and from respective variant without VX-809, respectively ($p<0.05$). (C) BHK cells expressing wt-, F508del-CFTR alone or jointly with ΔRI_L, ΔRE_S and ΔRI_L-ΔRE_S were subjected to pulse-chase (see Methods) for the indicated times (0, 0.5, 1, 2, 3h) before lysis and IP with the anti-CFTR 596 Ab. After electrophoresis and fluorography, images were analysed by densitometry. (D) Turnover of immature (band B) CFTR for different CFTR variants is shown as the percentage of immature protein at a given time point of chase (P_t) relative to the amount at t=0 (P_0). (E) Efficiency of processing of band B into band C is shown as the percentage of band C at a given time of chase relative to the amount of band B at t=0. "*" and "#" indicate statistical significantly different ($p<0.05$) from wt-CFTR and F508del-CFTR, respectively. Data represent mean ± SEM (n=5).

FIGURE 5. Functional characterization of the ΔRE_S and ΔRI_L variants of F508del-CFTR with or without VX-809 or VX-770 treatments. (A, B) Summary of data from the iodide efflux peak magnitude generated by BHK cells stably expressing different CFTR variants and treated with 3μM VX-809 (black bars on panel A) or with DMSO as control (white bars on panel a) for 48h and stimulated with 10μM Forskolin (Fsk) and 50μM Genistein (Gen). In (B) cells were not pre-incubated and were stimulated either with 10μM Fsk and 50μM Gen (white bars on panel B) or with 10μM Fsk and 10μM VX-770 (black bars on panel b), as indicated. Data are shown as a percentage of wt-CFTR activity under Fsk/Gen stimulation and as mean±SEM . (n) indicates no. of independent experiments. "#" indicates significantly different ($p<0.05$) from the same CFTR variant incubated with DMSO (A) or significantly different from the same CFTR variant under Fsk/Gen stimulation (white bars) (B). (C) Summary of iodide efflux data for different F508del-CFTR variants without RE_S, RI_S, RI_L alone or jointly with revertants R1070W and G550E.

FIGURE 6. Summary of the most relevant results observed in the present study. CFTR structure used is the one by Liu F *et al* [33] and putative bind sites of VX-809 and VX-770 shown are the NBD1:MSD2 (ICL4) interface and to the MSDs (although it is not defined the exact binding site), as described by Farinha *et al* [41] and by Jih & Hwang [42], respectively.

#

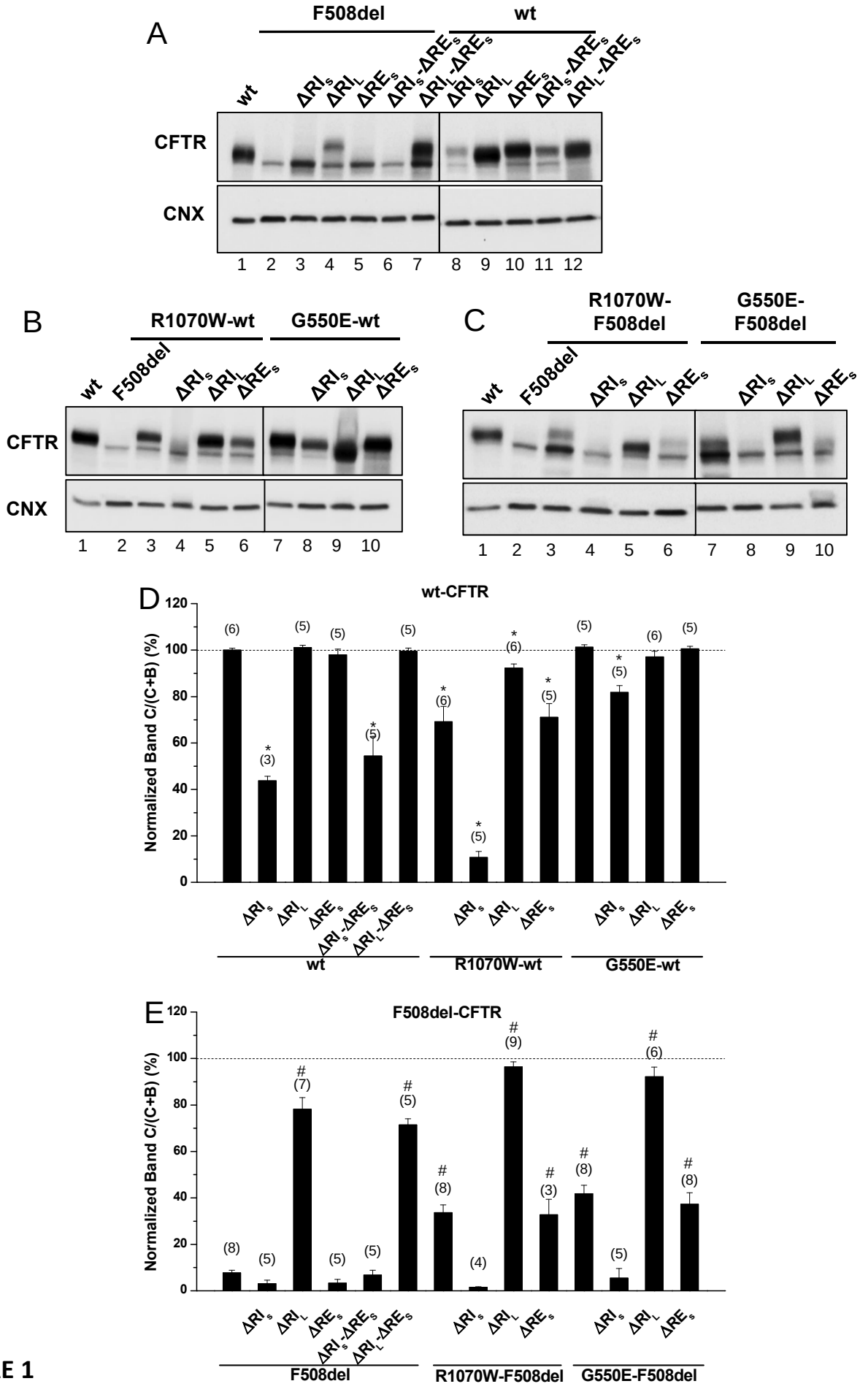
A
F508del
wt
wt
ΔRIs
ΔRIL
ΔREs
ΔRIs-ΔREs
ΔRIL-ΔREs
CFTR
CNX
1 2 3 4 5 6 7 8 9 10 11 12
B
R1070W-wt
G550E-wt
wt
F508del
ΔRIs
ΔRIL
ΔREs
CFTR
CNX
1 2 3 4 5 6 7 8 9 10
C
R1070W-F508del
G550E-F508del
wt
F508del
ΔRIs
ΔRIL
ΔREs
1 2 3 4 5 6 7 8 9 10
D
wt-CFTR
Normalized Band C/(C+B) (%)
ΔRIs
ΔRIL
ΔREs
ΔRIs-ΔREs
ΔRIL-ΔREs
wt
R1070W-wt
G550E-wt
E
F508del-CFTR
Normalized Band C/(C+B) (%)
F508del
R1070W-F508del
G550E-F508del

FIGURE 1

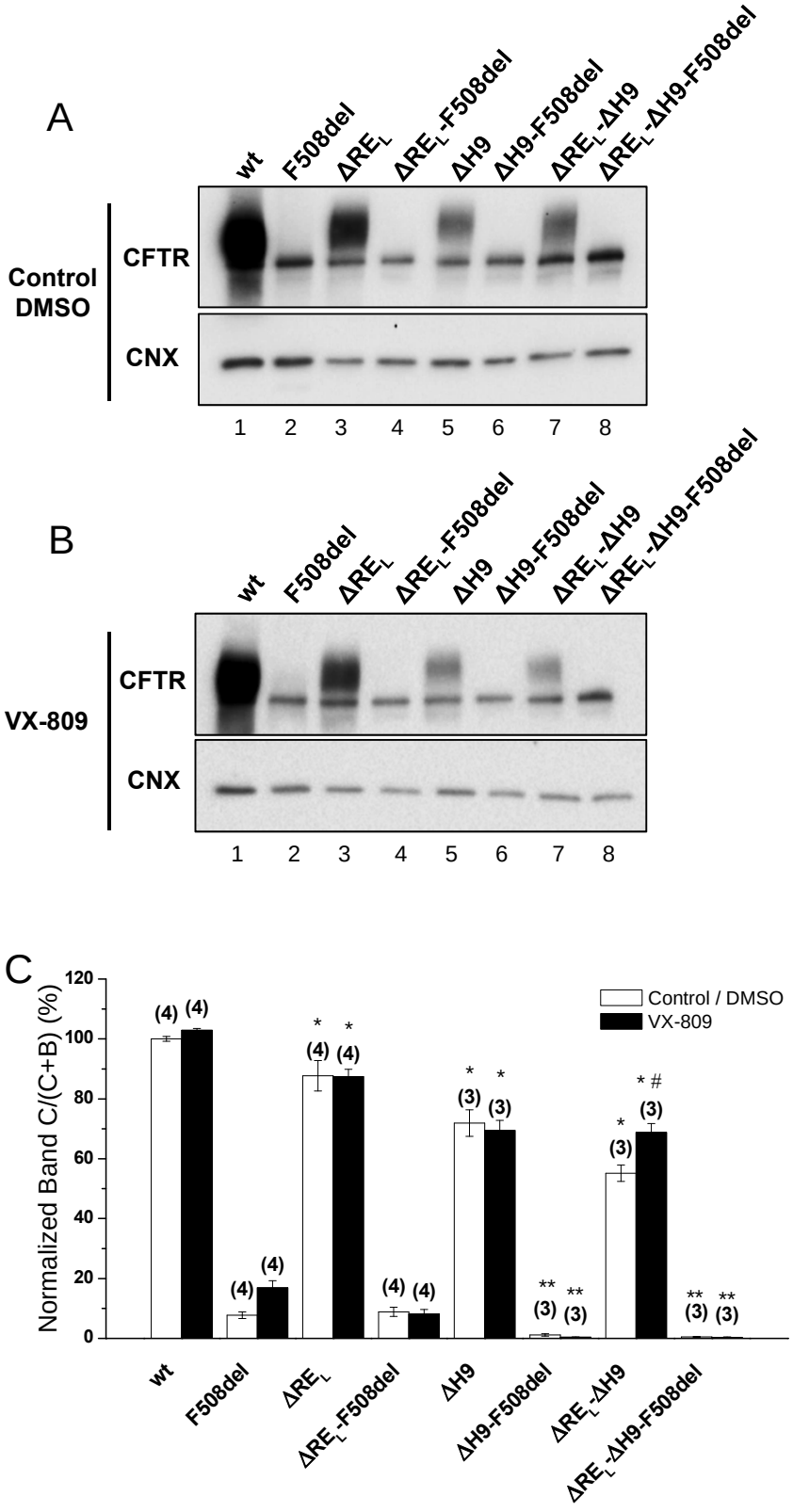
A
wt
F508del
ΔRE_L
ΔRE_L-F508del
ΔH9
ΔH9-F508del
ΔRE_L-ΔH9
ΔRE_L-ΔH9-F508del
Control DMSO
CFTR
CNX
1 2 3 4 5 6 7 8
B
VX-809
C
Normalized Band C/(C+B) (%)
Control / DMSO
VX-809

FIGURE 2

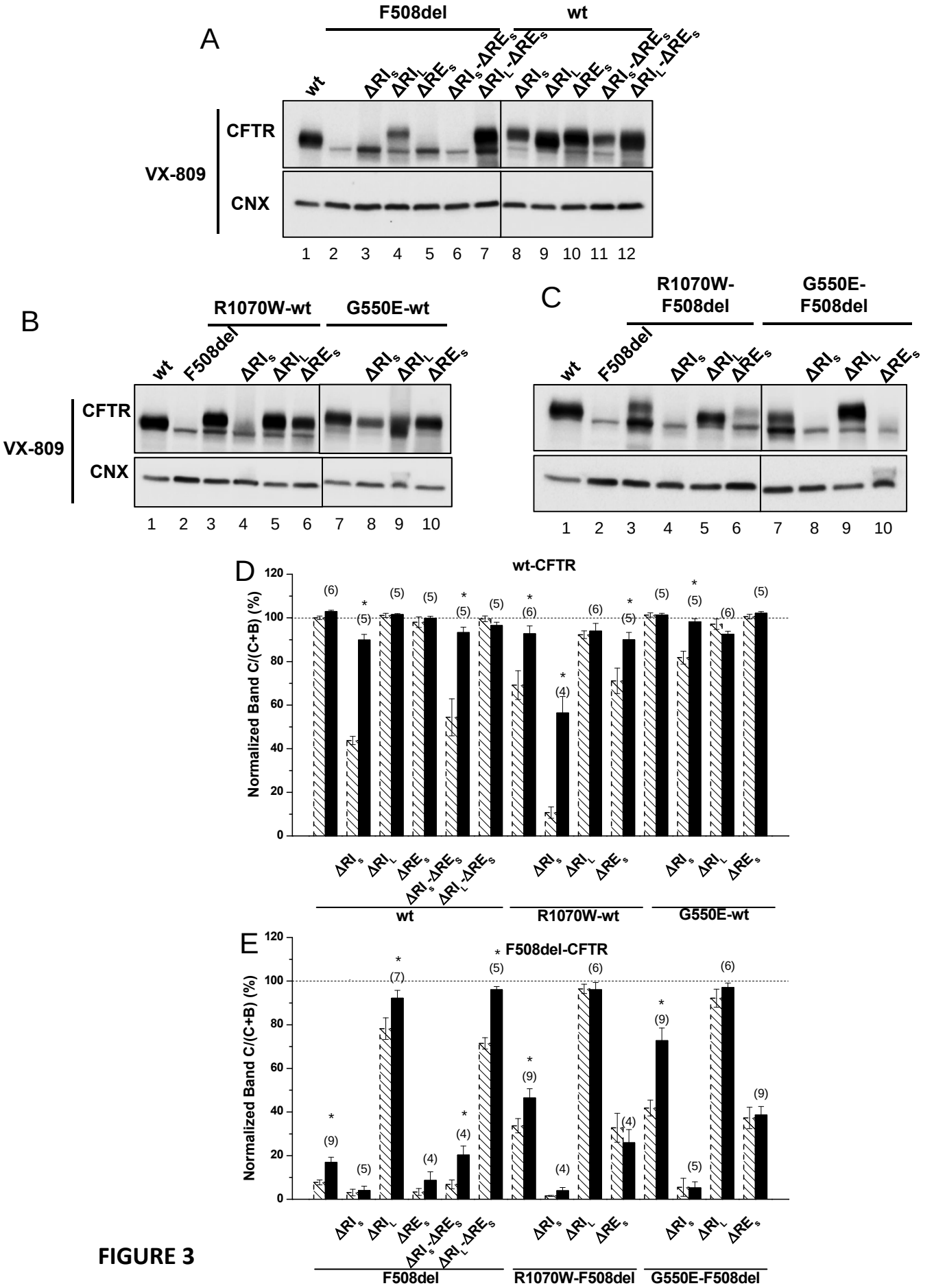
A
F508del
wt
wt
ΔRIs
ΔRIL
ΔREs
ΔRIs-ΔREs
ΔRIL-ΔREs
VX-809
CFTR
CNX
1 2 3 4 5 6 7 8 9 10 11 12
B
R1070W-wt
G550E-wt
wt
F508del
VX-809
CFTR
CNX
1 2 3 4 5 6 7 8 9 10
C
R1070W-F508del
G550E-F508del
1 2 3 4 5 6 7 8 9 10
D
wt-CFTR
Normalized Band C/(C+B) (%)
wt
R1070W-wt
G550E-wt
E
F508del-CFTR
Normalized Band C/(C+B) (%)
F508del
R1070W-F508del
G550E-F508del

FIGURE 3

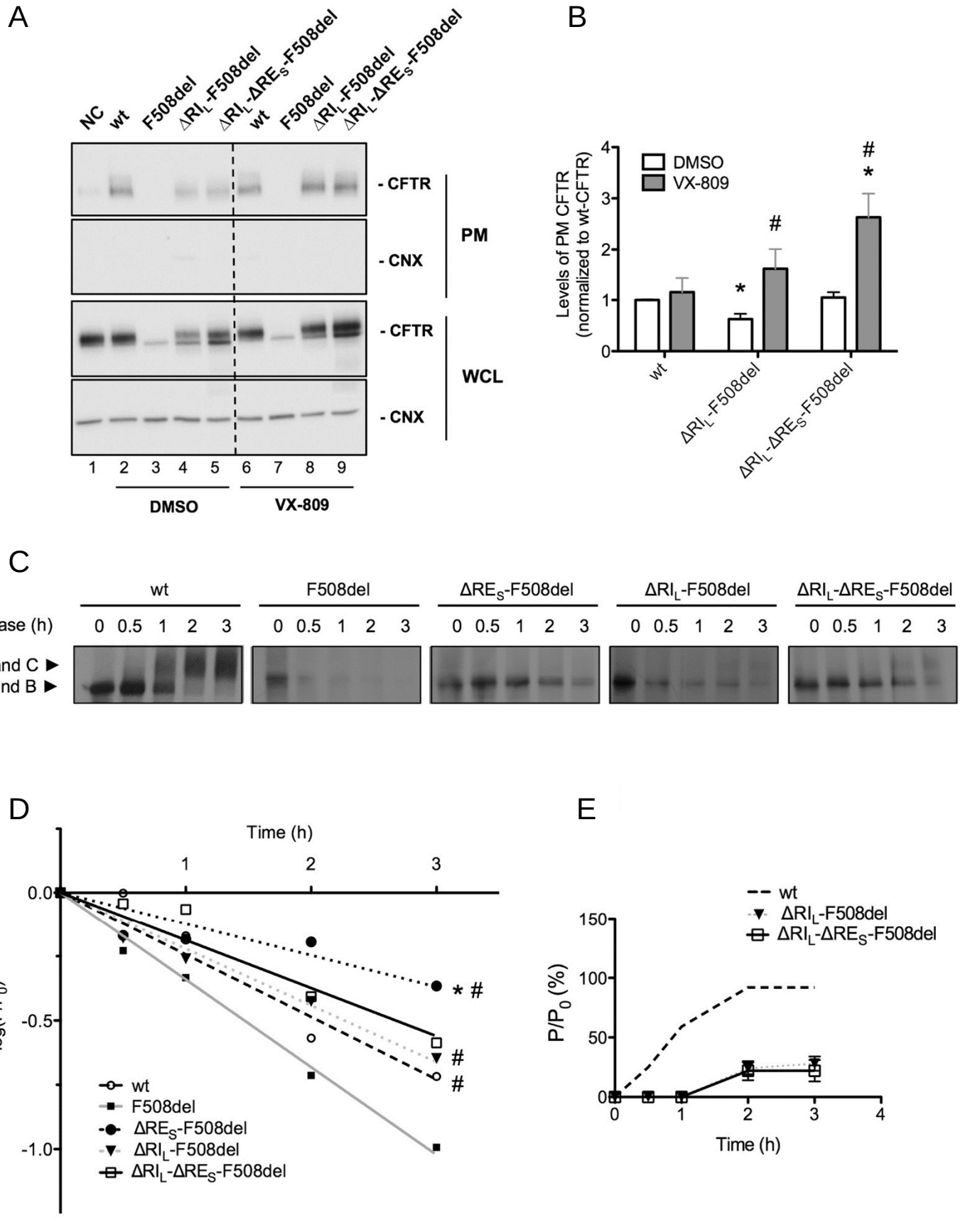
A
NC
wt
F508del
ΔRI$_L$-F508del
ΔRI$_L$-ΔRE$_S$-F508del
wt
F508del
ΔRI$_L$-F508del
ΔRI$_L$-ΔRE$_S$-F508del
- CFTR
- CNX
PM
- CFTR
- CNX
WCL
1 2 3 4 5 6 7 8 9
DMSO
VX-809
B
DMSO
VX-809
Levels of PM CFTR (normalized to wt-CFTR)
wt
ΔRI$_L$-F508del
ΔRI$_L$-ΔRE$_S$-F508del
C
wt
F508del
ΔRE$_S$-F508del
ΔRI$_L$-F508del
ΔRI$_L$-ΔRE$_S$-F508del
Chase (h)
0 0.5 1 2 3
Band C
Band B
D
Time (h)
log(P/P$_0$)
wt
F508del
ΔRE$_S$-F508del
ΔRI$_L$-F508del
ΔRI$_L$-ΔRE$_S$-F508del
E
P/P$_0$ (%)
Time (h)
wt
ΔRI$_L$-F508del
ΔRI$_L$-ΔRE$_S$-F508del

FIGURE 4

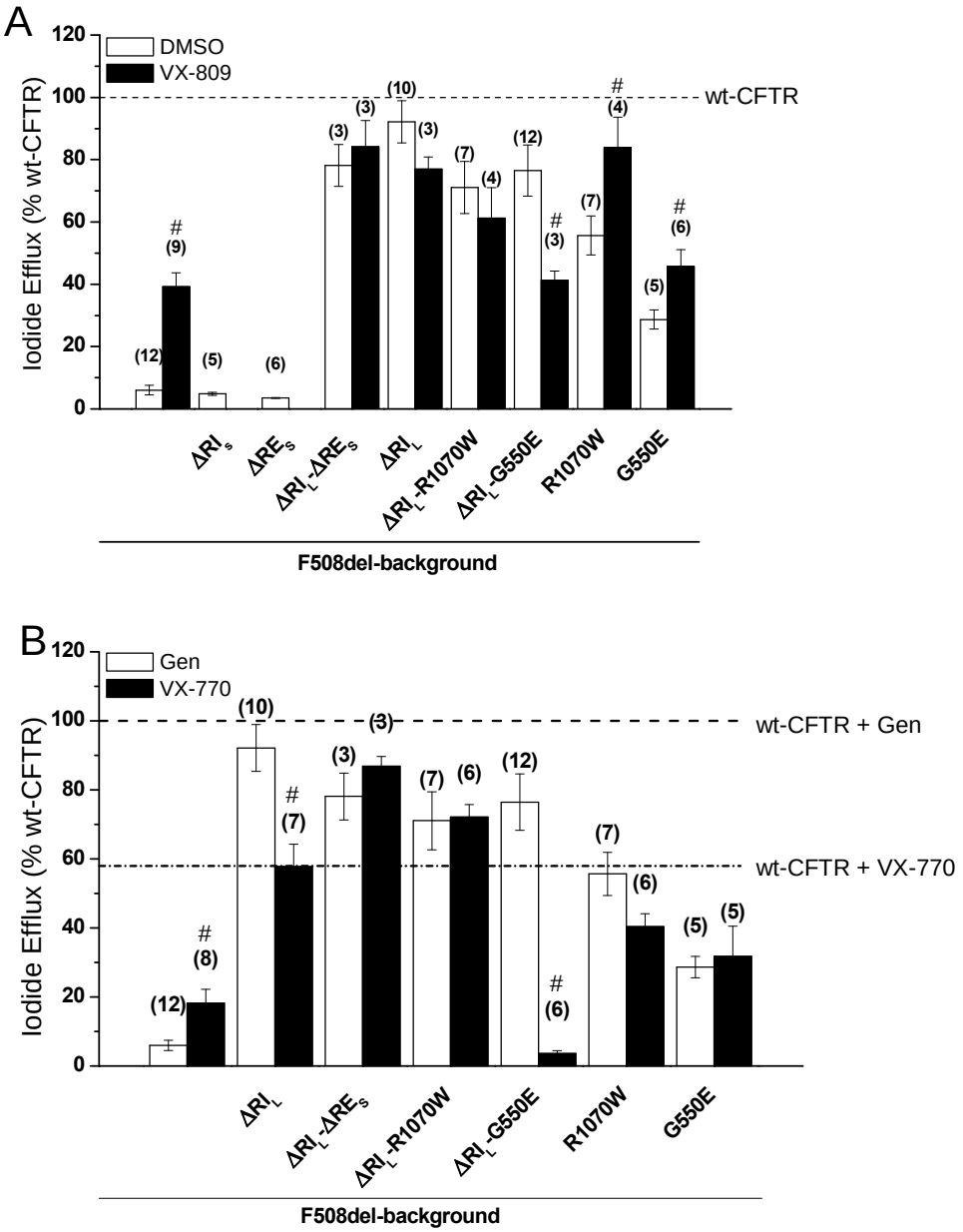

C

CFTR variant	DMSO			VX-809			VX-770		
	peak (min)	value	% to control wt-CFTR	peak (min)	value	% to control wt-CFTR	peak (min)	value	% to control wt-CFTR
wt	2	51 ± 3	100 ± 5	2	51 ± 4	100 ± 8	2	30 ± 4	58 ± 9
F508del	4	3 ± 1	6 ± 1	4	20 ± 2	39 ± 4	4	9 ± 2	18 ± 4
ΔRI$_S$-F508del	-	2 ± 0	5 ± 0	-	-	-	-	-	-
ΔRE$_S$-F508del	-	2 ± 0	3 ± 0	-	-	-	-	-	-
ΔRI$_L$-ΔRE$_S$-F508del	3	40 ± 3	78 ± 7	2	43 ± 4	84 ± 8	2	44 ± 1	87 ± 3
ΔRI$_L$-F508del	3	47 ± 3	92 ± 7	3	39 ± 2	77 ± 4	3	30 ± 3	58 ± 7
ΔRI$_L$-R1070W-F508del	2	36 ± 4	71 ± 8	2	31 ± 5	61 ± 10	1	37 ± 2	72 ± 4
ΔRI$_L$-G550E-F508del	2	39 ± 4	76 ± 8	2	21 ± 2	41 ± 3	-	2 ± 0	4 ± 1
R1070W-F508del	2	28 ± 3	56 ± 6	2	43 ± 5	84 ± 10	3	21 ± 2	40 ± 4
G550E-F508del	2	15 ± 2	29 ± 3	2	23 ± 3	46 ± 5	3	16 ± 4	32 ± 9

FIGURE 5

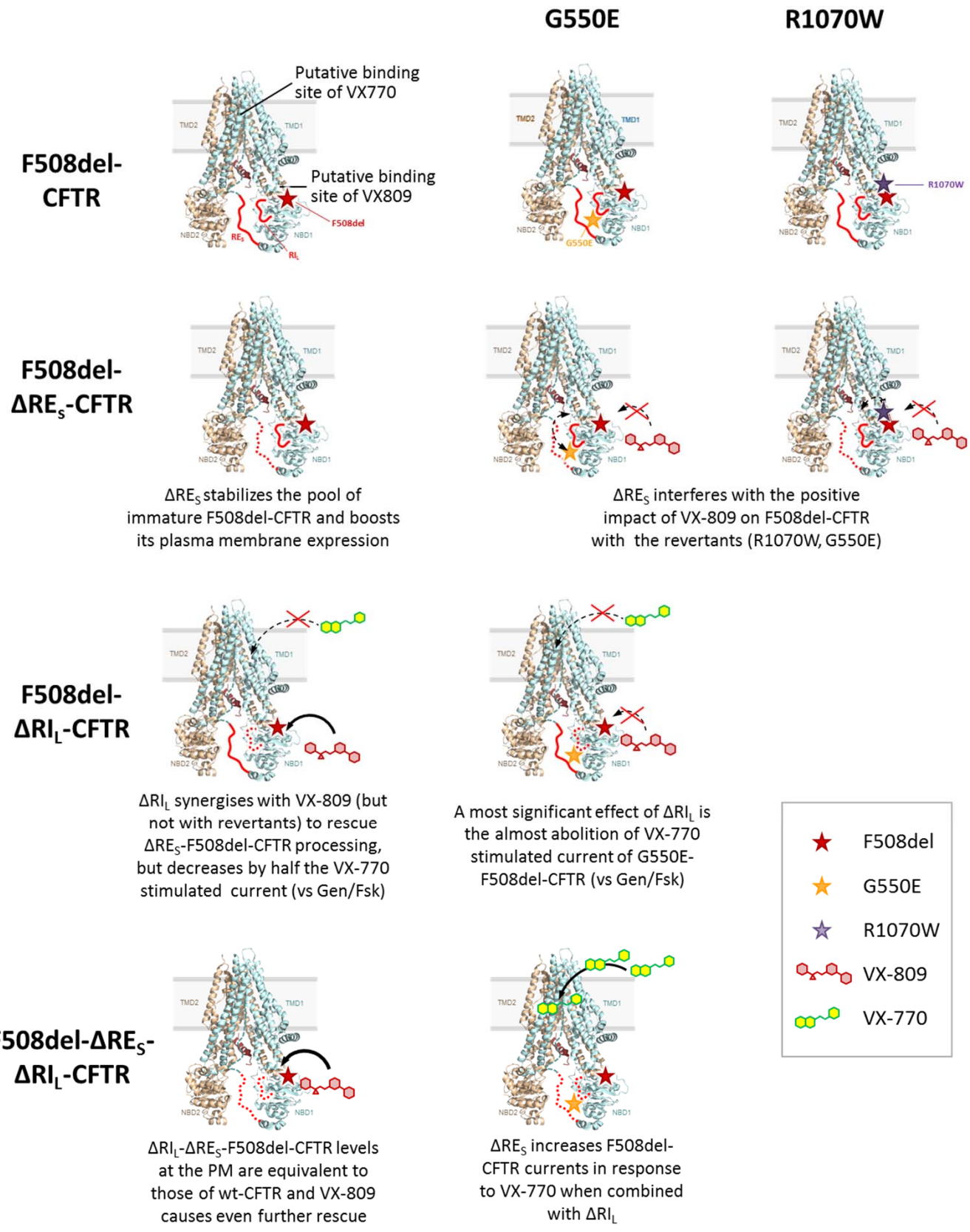
G550E
R1070W
F508del-CFTR
Putative binding site of VX770
Putative binding site of VX809
F508del
R1070W
G550E
F508del-ΔRE$_S$-CFTR
ΔRE$_S$ stabilizes the pool of immature F508del-CFTR and boosts its plasma membrane expression
ΔRE$_S$ interferes with the positive impact of VX-809 on F508del-CFTR with the revertants (R1070W, G550E)
F508del-ΔRI$_L$-CFTR
ΔRI$_L$ synergises with VX-809 (but not with revertants) to rescue ΔRE$_S$-F508del-CFTR processing, but decreases by half the VX-770 stimulated current (vs Gen/Fsk)
A most significant effect of ΔRI$_L$ is the almost abolition of VX-770 stimulated current of G550E-F508del-CFTR (vs Gen/Fsk)
F508del
G550E
R1070W
VX-809
VX-770
F508del-ΔRE$_S$-ΔRI$_L$-CFTR
ΔRI$_L$-ΔRE$_S$-F508del-CFTR levels at the PM are equivalent to those of wt-CFTR and VX-809 causes even further rescue
ΔRE$_S$ increases F508del-CFTR currents in response to VX-770 when combined with ΔRI$_L$

FIGURE 6